International Scholarly Research Network
ISRN Signal Processing
Volume 2012, Article ID 121628, 17 pages
doi:10.5402/2012/121628

*Research Article*

# Towards Modal Integration of Overhead and Underground Low-Voltage and Medium-Voltage Power Line Communication Channels in the Smart Grid Landscape: Model Expansion, Broadband Signal Transmission Characteristics, and Statistical Performance Metrics (Invited Paper)

**Athanasios G. Lazaropoulos**

*School of Electrical and Computer Engineering, National Technical University of Athens, 9 Iroon Polytechniou Street, Zografou, 15780 Athens, Greece*

Correspondence should be addressed to Athanasios G. Lazaropoulos, aglazaropoulos@gmail.com

Received 26 March 2012; Accepted 8 May 2012

Academic Editors: L. Shen and M. Wicks



The established statistical analysis, already used to treat overhead transmission power grid networks, is now implemented to examine the factors influencing modal transmission characteristics and modal statistical performance metrics of overhead and underground low-voltage/broadband over power lines (LV/BPL) and medium-voltage/broadband over power lines (MV/BPL) channels associated with power distribution in smart grid (SG) networks. The novelty of this paper is threefold. First, a refined multidimensional chain scattering matrix (TM2) method suitable for overhead and underground LV/BPL and MV/BPL modal channels is evaluated against other relative theoretical and experimental proven models. Second, applying TM2 method, the end-to-end modal channel attenuation of various LV/BPL and MV/BPL multiconductor transmission line (MTL) configurations is determined. The LV/BPL and MV/BPL transmission channels are investigated with regard to their spectral behavior and their end-to-end modal channel attenuation. It is found that the above features depend drastically on the frequency, the type of power grid, the mode considered, the MTL configuration, the physical properties of the cables used, the end-to-end distance, and the number, the electrical length, and the terminations of the branches encountered along the end-to-end BPL signal propagation. Third, the statistical properties of various overhead and underground LV/BPL and MV/BPL modal channels are investigated revealing the correlation between end-to-end modal channel attenuation and modal root-mean-square delay spread (RMS-DS). Already verified in the case of overhead high-voltage (HV) BPL systems, this fundamental property of several wireline systems is also modally validated against relevant sets of field measurements, numerical results, and recently proposed statistical channel models for various overhead and underground LV/BPL and MV/BPL channels. Based on this common inherent attribute of either transmission or distribution BPL networks, new unified regression trend line is proposed giving a further boost towards BPL system intraoperability. A consequence of this paper is that it aids in gaining a better understanding of the range and coverage that BPL solutions can achieve; a preliminary step toward the system symbiosis between BPL systems and other broadband technologies in an SG environment.

## 1. Introduction

The topic of this work is the use of the low-voltage (LV) and medium-voltage (MV) distribution power grids as a transmission medium for broadband communications. This kind of technology is known as broadband over power lines (BPL), and it is not only a promising solution for delivering broadband last mile access in remote and/or underdeveloped areas but also the key to developing an advanced IP-based power system, offering a plethora of potential smart grid (SG) applications [1–3].

Utilities employ either the overhead or the underground distribution power grid for new urban, suburban, and rural LV and MV installations. The choice is made according to different criteria like cost requirements, existing grid topology, and urban plan constraints [4–6].

When considered as a transmission medium for communication signals, the overhead and underground LV and MV power grids are subjected to attenuation, multipath due to various reflections, noise, and electromagnetic interference [7–14]. Each of the aforementioned adverse factors critically affects the overall performance and the design of BPL systems [15–18].

Due to the need of broadband communications through distribution power grids, the development of accurate channel models at high frequencies along the overhead and underground LV and MV distribution power lines is imperative. As usually done in BPL transmission, a hybrid model is employed to examine the behavior of BPL transmission channels installed on BPL multiconductor transmission line (MTL) structures [1, 8–11, 19–28]. Through a bottom-up approach consisting of an appropriate combination of the similarity transformation and MTL theory, the modes that may be supported by a BPL configuration are determined concerning their propagation constants and their characteristic impedances [1, 8, 22–32]. In this paper, a top-down approach, is proposed to determine the end-to-end attenuation of overhead and underground LV/BPL and MV/BPL modal channels. Based on an exact version of multidimensional chain scattering matrix or T-Matrix method, this novel extended T-Matrix (TM2) method combines the accuracy of the generic multidimensional network analysis tool presented in [22–24] and the simplicity of hybrid model of [8–11, 19–21]. The influence of factors, such as the physical properties of the cables used, the MTL configuration, the end-to-end distance, and the number, the electrical length, and the terminations of the branches encountered along the end-to-end BPL signal propagation are investigated based on numerical results concerning simulated overhead and underground LV/BPL and MV/BPL topologies.

On the basis of these numerical results, statistical properties of BPL modal channels are reported. The common nature of overhead and underground LV/BPL and MV/BPL transmission lines is mirrored on important statistical performance metrics, such as the attenuation exceedance probability, the average end-to-end attenuation, and the root-mean-square delay spread (RMS-DS) of BPL modal channels. Specifically, it is confirmed that average end-to-end channel attenuation and RMS-DS in overhead and underground LV/BPL and MV/BPL modal channels are positively correlated lognormal random variables being in agreement with: (i) relevant sets of measurements and relevant distributions of recently proposed statistical BPL channel models [33–41]; (ii) recent simulation results regarding various overhead HV/BPL channels [19]. Since this inherent statistical characteristic is validated in the cases of overhead and underground LV/BPL, MV/BPL, and HV/BPL power grids, a suitable unified approximation is proposed—UNI[1] regression trend line—that commonly describes either BPL distribution or transmission power grids enhancing the common handling of BPL networks in an SG landscape.

The rest of this paper is organized as follows. In Section 2, the modal behavior of BPL propagation is discussed along with the necessary assumptions concerning overhead and underground LV/BPL and MV/BPL transmission. Section 3 deals with signal transmission via power lines by the TM2 method which is applied for the evaluation of the end-to-end modal transfer functions. Section 4 provides a description of the modal statistical performance metrics considered. In Section 5, numerical results are provided, aiming at marking out how the various features of the overhead and underground LV and MV distribution power grids influence BPL transmission and statistical performance metrics. Section 6 concludes the paper.

## 2. The Physical BPL Layer

The overhead and underground LV and MV distribution power grids differ considerably from signal transmission via twisted-pair, coaxial or fiber-optic cables due to the significant differences of the network structure and the physical properties of the power cables used [1, 5–8, 10, 15, 42].

*2.1. Overhead LV and MV Power Distribution Networks.* A typical case of overhead LV distribution line is depicted in Figure 1(a). Four parallel noninsulated conductors are suspended one above the other spaced by $\Delta_{\mathrm{LV}}$ in the range from 0.3 m to 0.5 m and located at heights $h_{\mathrm{LV}}$ ranging from 6 m to 10 m above ground for the lowest conductor. The upper conductor is the neutral, while the lower three conductors are the three phases. This three-phase four-conductor overhead LV distribution line configuration is considered in the present work consisting of ASTER $3 \times 54.6\,\mathrm{mm}^2 + 1 \times 34.4\,\mathrm{mm}^2$ conductors [4, 5, 30, 31, 43, 44].

Overhead MV distribution lines hang at typical heights $h_{\mathrm{MV}}$ ranging from 8 m to 10 m above ground. Typically, three parallel noninsulated phase conductors spaced by $\Delta_{\mathrm{MV}}$ in the range from 0.3 m to 1 m are used above lossy ground. This three-phase overhead MV distribution line configuration is considered in the present work consisting of ACSR $3 \times 95\,\mathrm{mm}^2$ conductors, see Figure 1(b)—[1, 4, 5, 8, 9, 42, 46].

The ground is considered as the reference conductor. The conductivity of the ground is assumed $\sigma_g = 5\,\mathrm{mS/m}$ and its relative permittivity $\varepsilon_{rg} = 13$, which is a realistic scenario [1, 8–10, 42].

The impact of imperfect ground on signal propagation over power lines was analyzed in [1, 8, 9, 42, 47–50]. This formulation has the advantage that, contrary to other available models for overhead power lines [44, 51–53], it is suitable for transmission at high frequencies above lossy ground and for broadband applications of overhead LV/BPL, MV/BPL, and HV/BPL systems.

*2.2. Underground LV and LV Power Distribution Networks.* The underground LV distribution line that will be examined in the simulations is the three-phase *HN33S33* underground

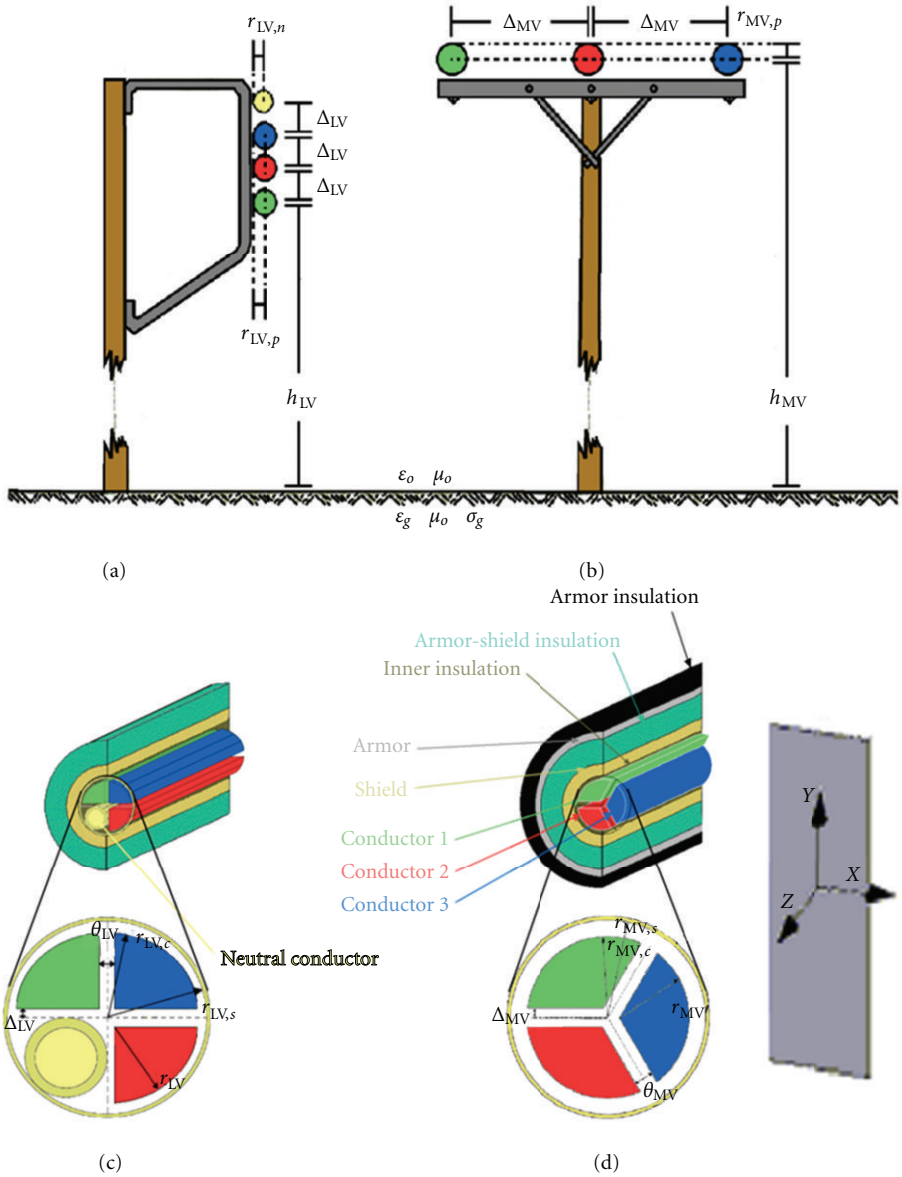


Figure 1: Typical multiconductor structures. (a) Overhead LV. (b) Overhead MV. (c) Underground LV. (d) Underground MV [8, 10, 22, 45].

LV distribution cable ($3 \times 150\,\text{mm}^2 + 1 \times 70\,\text{mm}^2$ Al, PVC, Steel-Pb shield). The layout of this cable is depicted in Figure 1(c). The cable arrangement consists of the three-phase three-sector-type conductors, one core-type neutral conductor, and one shield conductor grounded at both ends. The neutral conductor is in galvanic contact with the shield. Hence, the shield is obtained by its concatenation with the neutral conductor [4, 5, 22–24, 26, 43].

The underground MV distribution line that will be examined is the three-phase sector-type PILC distribution-class cable (8/10 kV, $3 \times 95\,\text{mm}^2$ Cu, PILC). The cable arrangement consists of the three-phase three-sector-type conductors, one shield conductor, and one armor conductor, see Figure 1(d). The shield and the armor are grounded at both ends [10, 54–57].

Due to the common practice of grounding at both ends, the shield acts as a ground return path and as a reference conductor and separates the inner conductors electrostatically and magnetostatically from the remaining set. Hence, the analysis may be focused only on the remaining four-conductor transmission line (TL) of interest consisting of the three phases and the shield. This is the common procedure either in theoretical analyses or in measurements [4–6, 10, 22–24, 26, 45, 54–60].

This paper focuses on broadband propagation via *HN33S33* underground LV distribution cable and the PILC underground MV distribution cable because: (i) in many countries, these types of cable are dominant in urban and suburban underground LV and MV power distribution installations, respectively [54, 55, 61–63]; (ii) the theoretical

results obtained concerning the propagation characteristics of the modes supported are found to be in excellent agreement with the experimental results obtained from the cable measurements [22–24, 26, 43, 54, 57]; (iii) the above LV and MV underground distribution cables—rather than other LV and MV underground cables which present lower attenuation—are studied because these types of cable behaves closer to the line-of-sight (LOS) transmission behavior (corresponding to "LOS" transmission in wireless channels) in the majority of existing underground LV and MV distribution grids. Thus, an indicative picture of the real world situation will be obtained [4, 6, 55].

Signal transmission via three-phase underground power lines has been analyzed in [10, 22–24, 26, 45, 64–67]. This formulation considers high frequency BPL transmission in the general case of underground power lines consisting of three-phase conductors with common shield and armor. It is suitable for transmission at high frequencies for broadband applications of underground LV/BPL and MV/BPL systems.

*2.3. Modal Analysis of Overhead and Underground LV/BPL and MV/BPL Systems.* Through a matrix approach, the standard TL analysis can be extended to the MTL case which involves more than two conductors. Compared to a two-conductor line supporting one forward- and one backward-traveling wave, an MTL structure with $n + 1$ conductors parallel to the $z$ axis as depicted in Figures 1(a), 1(b), 1(c), and 1(d) may support $n$ pairs of forward- and backward-traveling waves with corresponding propagation constants. These waves may be described by a coupled set of $2n$ first-order partial differential equations relating the line voltages $V_i(z,t)$, $i = 1,\ldots,n$ to the line currents $I_i(z,t)$, $i = 1,\ldots,n$. Each pair of forward- and backward-traveling waves is referred to as a mode [1, 8, 10, 19–21, 29–31, 42].

By extending the modal analysis to examine signal transmission via overhead and underground LV and MV distribution power cables, it was found out that $n$ modes may be supported, namely: (i) the common mode (CM) which propagates via the $n$ conductors and returns via the ground or the shield for overhead or underground BPL systems, respectively; (ii) the $n - 1$ differential modes ($\mathrm{DM}_{i-1}$, $i = 2,\ldots,n$) which propagate and return via the $n$ conductors. In the overhead case, $\gamma_{\mathrm{CM}}^{\mathrm{OV,LV}}$, $\gamma_{\mathrm{DM}i-1}^{\mathrm{OV,LV}}$, $i = 2,3,4$, $\gamma_{\mathrm{CM}}^{\mathrm{OV,MV}}$, and $\gamma_{\mathrm{DM}j-1}^{\mathrm{OV,MV}}$, $j = 2,3$ constitute the propagation constants of overhead LV/BPL CM ($\mathrm{CM}^{\mathrm{OV,LV}}$), overhead LV/BPL DMs ($\mathrm{DM}^{\mathrm{OV,LV}}s$), overhead MV/BPL CM ($\mathrm{CM}^{\mathrm{OV,MV}}$), and overhead MV/BPL DMs ($\mathrm{DM}^{\mathrm{OV,MV}}s$), respectively [1, 4, 5, 8, 22–24, 26, 30, 31, 42, 43, 47–50]. Similarly, in the underground case, $\gamma_{\mathrm{CM}}^{\mathrm{UN,LV}}$, $\gamma_{\mathrm{DM}i-1}^{\mathrm{UN,LV}}$ $i = 2,3$, $\gamma_{\mathrm{CM}}^{\mathrm{UN,MV}}$, and $\gamma_{\mathrm{DM}j-1}^{\mathrm{UN,MV}}$ $j = 2,3$ constitute the propagation constants of underground LV/BPL CM ($\mathrm{CM}^{\mathrm{UN,LV}}$), underground LV/BPL DMs ($\mathrm{DM}^{\mathrm{UN,LV}}s$), underground MV/BPL CM ($\mathrm{CM}^{\mathrm{UN,MV}}$), and underground MV/BPL DMs ($\mathrm{DM}^{\mathrm{UN,MV}}s$), respectively [8–11, 22–24, 26, 30, 31, 43, 54–57, 68].

The attenuation coefficients $\alpha_{\mathrm{CM}}^{\mathrm{OV,LV}} = \mathrm{Re}\{\gamma_{\mathrm{CM}}^{\mathrm{OV,LV}}\}$, $\alpha_{\mathrm{DM}i-1}^{\mathrm{OV,LV}} = \mathrm{Re}\{\gamma_{\mathrm{DM}i-1}^{\mathrm{OV,LV}}\}$ $i = 2,3,4$, $\alpha_{\mathrm{CM}}^{\mathrm{UN,LV}} = \mathrm{Re}\{\gamma_{\mathrm{CM}}^{\mathrm{UN,LV}}\}$, and $\alpha_{\mathrm{DM}j-1}^{\mathrm{UN,LV}} = \mathrm{Re}\{\gamma_{\mathrm{DM}j-1}^{\mathrm{UN,LV}}\}$ $j = 2,3$ of the $\mathrm{CM}^{\mathrm{OV,LV}}$, the three $\mathrm{DM}^{\mathrm{OV,LV}}s$, the $\mathrm{CM}^{\mathrm{UN,LV}}$, and the two $\mathrm{DM}^{\mathrm{UN,LV}}s$ are plotted versus frequency in Figure 2(a) for the overhead and underground LV/BPL configurations depicted in Figures 1(a) and 1(c), respectively. In Figure 2(b), the attenuation coefficients $\alpha_{\mathrm{CM}}^{\mathrm{OV,MV}} = \mathrm{Re}\{\gamma_{\mathrm{CM}}^{\mathrm{OV,MV}}\}$, $\alpha_{\mathrm{DM}p-1}^{\mathrm{OV,MV}} = \mathrm{Re}\{\gamma_{\mathrm{DM}p-1}^{\mathrm{OV,MV}}\}$ $p = 2,3$, $\alpha_{\mathrm{CM}}^{\mathrm{UN,MV}} = \mathrm{Re}\{\gamma_{\mathrm{CM}}^{\mathrm{UN,MV}}\}$, and $\alpha_{\mathrm{DM}q-1}^{\mathrm{UN,MV}} = \mathrm{Re}\{\gamma_{\mathrm{DM}q-1}^{\mathrm{UN,MV}}\}$ $q = 2,3$ of $\mathrm{CM}^{\mathrm{OV,MV}}$, the two $\mathrm{DM}^{\mathrm{OV,MV}}s$, $\mathrm{CM}^{\mathrm{UN,MV}}$, and the two $\mathrm{DM}^{\mathrm{UN,MV}}s$ DMs are plotted with respect to frequency for the overhead and underground MV/BPL configurations depicted in Figures 1(b) and 1(d), respectively. The phase delays $\beta_{\mathrm{CM}}^{\mathrm{OV,LV}} = \mathrm{Im}\{\gamma_{\mathrm{CM}}^{\mathrm{OV,LV}}\}$, $\beta_{\mathrm{DM}i-1}^{\mathrm{OV,LV}} = \mathrm{Im}\{\gamma_{\mathrm{DM}i-1}^{\mathrm{OV,LV}}\}$ $i = 2,3,4$, $\beta_{\mathrm{CM}}^{\mathrm{UN,LV}} = \mathrm{Im}\{\gamma_{\mathrm{CM}}^{\mathrm{UN,LV}}\}$, $\beta_{\mathrm{DM}p-1}^{\mathrm{UN,LV}} = \mathrm{Im}\{\gamma_{\mathrm{DM}p-1}^{\mathrm{UN,LV}}\}$ $p = 2,3$, $\beta_{\mathrm{CM}}^{\mathrm{OV,MV}} = \mathrm{Im}\{\gamma_{\mathrm{CM}}^{\mathrm{OV,MV}}\}$, $\beta_{\mathrm{DM}j-1}^{\mathrm{OV,MV}} = \mathrm{Im}\{\gamma_{\mathrm{DM}j-1}^{\mathrm{OV,MV}}\}$ $j = 2,3$, $\beta_{\mathrm{CM}}^{\mathrm{UN,MV}} = \mathrm{Im}\{\gamma_{\mathrm{CM}}^{\mathrm{UN,MV}}\}$, and $\beta_{\mathrm{DM}q-1}^{\mathrm{UN,MV}} = \mathrm{Im}\{\gamma_{\mathrm{DM}q-1}^{\mathrm{UN,MV}}\}$ $q = 2,3$ of the $\mathrm{CM}^{\mathrm{OV,LV}}$, the three $\mathrm{DM}^{\mathrm{OV,LV}}s$, the $\mathrm{CM}^{\mathrm{UN,LV}}$, the two $\mathrm{DM}^{\mathrm{UN,LV}}s$, $\mathrm{CM}^{\mathrm{OV,MV}}$, the two $\mathrm{DM}^{\mathrm{OV,MV}}s$, $\mathrm{CM}^{\mathrm{UN,MV}}$, and the two $\mathrm{DM}^{\mathrm{UN,MV}}s$, respectively, (not plotted in this paper) are linear functions of frequency [1, 8, 9, 19–21, 42, 47–50, 54, 56, 57, 68].

As it has already been presented in [8–11, 19–21], the modal voltages $\mathbf{V}^m(z) = [V_1^m(z) \cdots V_n^m(z)]^T$ and the modal currents $\mathbf{I}^m(z) = [I_1^m(z) \cdots I_n^m(z)]^T$ may be related to the respective line quantities $\mathbf{V}(z) = [V_1(z) \cdots V_n(z)]^T$ and $\mathbf{I}(z) = [I_1(z) \cdots I_n(z)]^T$ via the similarity transformations [8, 10, 19–22, 30, 31]

$$\mathbf{V}(z) = \mathbf{T}_V \cdot \mathbf{V}^m(z), \tag{1}$$

$$\mathbf{I}(z) = \mathbf{T}_I \cdot \mathbf{I}^m(z), \tag{2}$$

where $[]^T$ denotes the transpose of a matrix, $\mathbf{T}_V$ and $\mathbf{T}_I$ are $n \times n$ matrices depending on the frequency, the physical properties of the cables, and the geometry of the MTL configuration [8, 10, 19–22, 30, 31]. Through the aforementioned equations, the line voltages and currents are expressed as appropriate superpositions of the respective modal quantities. From (1)

$$\mathbf{V}^m(0) = \mathbf{T}_V^{-1} \cdot \mathbf{V}(0). \tag{3}$$

The TM2 method—considered in Section 3—models the spectral relationship between $V_i^m(z)$, $i = 1,\ldots,n$ and $V_i^m(0)$, $i = 1,\ldots,n$ proposing operators $H_{i,j}^m\{\cdot\}$, $i,j = 1,\ldots,n$ so that

$$\mathbf{V}^m(z) = \mathbf{H}^m\{\mathbf{V}^m(0)\}, \tag{4}$$

where $\mathbf{H}^m\{\cdot\}$ is a $n \times n$ matrix operator whose elements $H_{i,j}^m\{\cdot\}$, $i,j = 1,\ldots,n$ with $i = j$ are the modal cochannel (CC) transfer functions, while those $H_{i,j}^m\{\cdot\}$, $i,j = 1,\ldots,n$ with $i \neq j$ are the modal cross-channel (XC) transfer functions and $H_{i,j}^m$ denotes the element of matrix $\mathbf{H}^m\{\cdot\}$ in row $i$ of column $j$. From (1), the $n \times n$ matrix channel transfer function $\mathbf{H}\{\cdot\}$ relating $\mathbf{V}(z)$ with $\mathbf{V}(0)$ through

$$\mathbf{V}(z) = \mathbf{H}\{\mathbf{V}(0)\} \tag{5}$$

is determined from

$$\mathbf{H}\{\cdot\} = \mathbf{T}_V \cdot \mathbf{H}^m\{\cdot\} \cdot \mathbf{T}_V^{-1}. \tag{6}$$

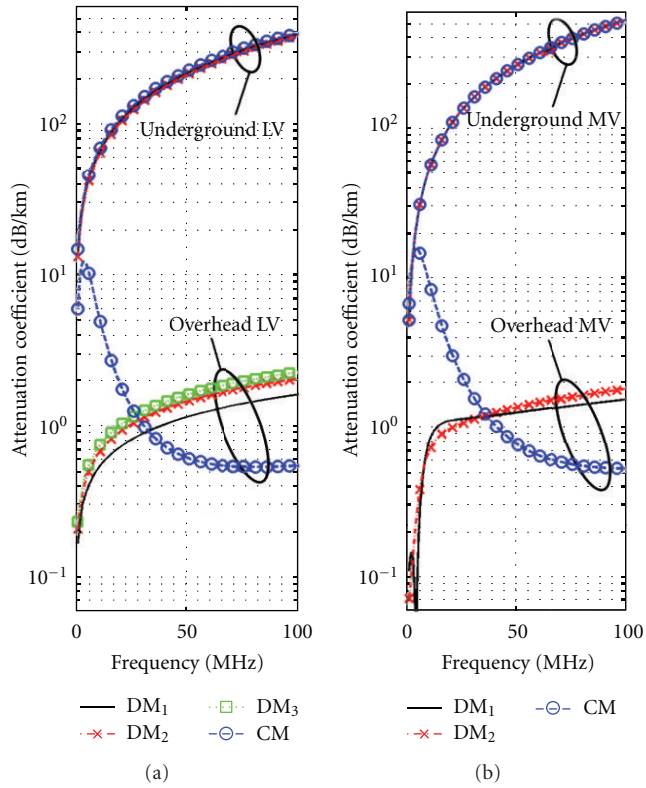


Figure 2: Frequency spectra of attenuation coefficients of BPL power distribution networks (the subchannel frequency span is equal to 0.1 MHz and logarithmic scale is used for the $y$-axes). (a) Overhead and underground LV. (b) Overhead and underground MV.

Based on (6), the $n \times n$ matrix transfer function $\mathbf{H}\{\cdot\}$ of the BPL distribution networks is determined.

## 3. Evaluation of the End-to-End Modal Transfer Functions

So far, several methods with converging results have been used to determine the modal transfer functions of BPL transmission channels [8–11, 19–24, 43, 69, 70]. In this paper, based on the well-established hybrid model of [8–11, 19–21] and the generic multidimensional network analysis of [22–24], the TM2 method is demonstrated. TM2 method constitutes a refined exact version of scattering matrix (SM) and TM methods—analyzed in [8–11, 19–21]—and is validated in overhead and underground LV/BPL and MV/BPL networks.

More specifically, similarly to TM method, in order to apply the TM2 method, an end-to-end BPL connection is separated into segments—network modules—, each of them comprising the successive branches encountered—see Figure 3(a). Signal transmission through the various network modules is taken into account based on the concatenation of respective chain scattering or T-matrices. A typical overhead or underground LV/BPL or MV/BPL end-to-end connection comprises branch-type network modules, as depicted in Figure 3(b), while A and B are assumed matched [1, 6, 8–11, 16, 19–21, 42, 48].

These "branch" modules may be considered as a cascade of two submodules. The multidimensional scattering characteristics of these two submodules—detailed in [22–24]—may be determined as follows.

(i) A "transmission" submodule representing a transmission line of length $L_k$ with the $2n^k \times 2n^k$ scattering matrix

$$\mathbf{S}^{T,k}\left(\gamma^k, L_k, \mathbf{U}^k\right) = \left[\begin{array}{c|c} \mathbf{S}_{11}^{T,k} & \mathbf{S}_{12}^{T,k} \\ \hline \mathbf{S}_{21}^{T,k} & \mathbf{S}_{22}^{T,k} \end{array}\right] = \left[\begin{array}{c|c} \mathbf{0}_{n^k \times n^k} & \mathbf{E}^{T,k} \\ \hline \mathbf{E}^{T,k} & \mathbf{0}_{n^k \times n^k} \end{array}\right], \quad (7)$$

where $\mathbf{E}^{T,k} = \operatorname{diag}\{\exp(-\gamma_1^k L_k) \cdots \exp(-\gamma_n^k L_k)\}$ is the corresponding $n^k \times n^k$ diagonal transmission matrix, $\mathbf{0}_{n^k \times n^k}$ is an $n^k \times n^k$ matrix with zero elements, and $\mathbf{S}_{11}^{T,k}$, $\mathbf{S}_{12}^{T,k}$, $\mathbf{S}_{21}^{T,k}$, $\mathbf{S}_{22}^{T,k}$ are the matrix elements of the $\mathbf{S}^{T,k}$ as evaluated from (7). $\gamma^k$, $\mathbf{U}^k$, and $n^k$ are the set with elements the propagation constant of the modes, the eigenbase, and the number of conductors, respectively, characterizing this "transmission" submodule MTL configuration. Since one type of overhead and underground LV/BPL and MV/BPL configuration is used across the end-to-end BPL connection it is assumed that $\mathbf{U} \equiv \mathbf{U}^k$ and $n = n^k$ are the reference eigenbase and the reference number of conductors, respectively.

(i) A "shunt" submodule representing the cascade of: (a) an $n^{bk} \times n^{bk}$ reflection matrix $\mathbf{K}_{bk}(\mathbf{Z}_{bk})$ associated with the branch terminations; (b) an $2n^{bk} \times 2n^{bk}$

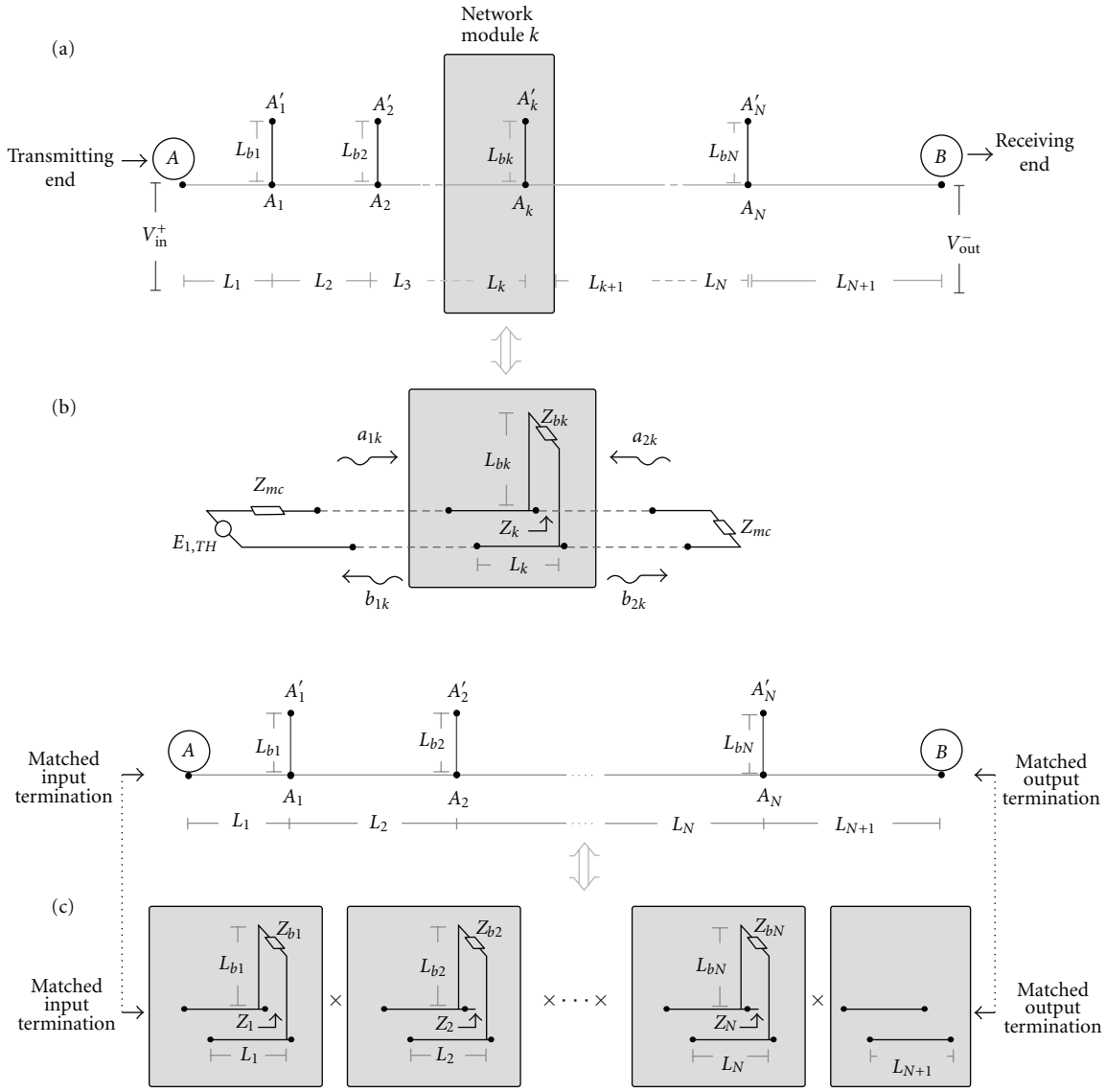


FIGURE 3: (a)End-to-end BPL connection with $N$ branches. (b) Network module. (c) An indicative BPL topology considered as a cascade of $N + 1$ modules corresponding to $N$ branches [8–11, 19–21].

scattering matrix $\mathbf{S}^{T,bk}(\gamma^{bk}, L_{bk}, \mathbf{U})$—similar expression to (7)—representing the branch transmission line of length $L_{bk}$; (c) an $n^{bk} \times n^k$ connection matrix $\mathbf{C}_k$ defining the interconnections between the transmission and branch conductors; with $2n^k \times 2n^k$ scattering matrix

$$\mathbf{S}^{S,k}\left(\gamma^{bk}, L_{bk}, \mathbf{U}\right) = \left[\begin{array}{c|c} \mathbf{S}_{11}^{S,k} & \mathbf{S}_{12}^{S,k} \\ \hline \mathbf{S}_{21}^{S,k} & \mathbf{S}_{22}^{S,k} \end{array}\right], \tag{8}$$

where $\mathbf{Z}_{bk}$ is the $n^{bk} \times n^{bk}$ branch termination matrix, $\mathbf{S}_{11}^{S,k}$, $\mathbf{S}_{12}^{S,k}$, $\mathbf{S}_{21}^{S,k}$, $\mathbf{S}_{22}^{S,k}$ are the matrix elements of the $\mathbf{S}^{S,k}$ matrix as determined from (8), and $\gamma^{bk}$ and $n^{bk}$ are the set with elements the propagation constant of the modes and the number of conductors, respectively, related to this "shunt" submodule MTL configuration [22–24]. Note that the number of conductors may vary from "transmission" to "shunt" submodules. Through the eigenbase change procedure—presented analytically in [22–24]—and by taking under consideration the reference eigenbase $\mathbf{U}$ and reference number of conductors $n$, scattering matrices $\mathbf{K}_{bk}$, $\mathbf{S}^{T,bk}$, and $\mathbf{C}_k$ may be grouped together through their cascading. Hence, the "shunt" scattering matrix of (8) may be evaluated.

Based on the specialized algebra for handling multidimensional scattering matrices presented in [71, 72] and by using (7) and (8), the $2n \times 2n$ "transmission" submodule chain

scattering matrix $\mathbf{T}^{T,k}$ and the $2n \times 2n$ "shunt" submodule chain scattering matrix $\mathbf{T}^{S,k}$ are determined by

$$\mathbf{T}^{T,k} = \left[\begin{array}{c|c} \mathbf{T}_{11}^{T,k} & \mathbf{T}_{12}^{T,k} \\ \hline \mathbf{T}_{21}^{T,k} & \mathbf{T}_{22}^{T,k} \end{array}\right] = \left[\begin{array}{c|c} \left[\mathbf{E}^{T,k}\right]^{-1} & \mathbf{0}_{n\times n} \\ \hline \mathbf{0}_{n\times n} & \mathbf{E}^{T,k} \end{array}\right], \tag{9}$$

$$\begin{aligned} \mathbf{T}^{S,k} &= \left[\begin{array}{c|c} \mathbf{T}_{11}^{S,k} & \mathbf{T}_{12}^{S,k} \\ \hline \mathbf{T}_{21}^{S,k} & \mathbf{T}_{22}^{S,k} \end{array}\right] \\ &= \left[\begin{array}{c|c} \left[\mathbf{S}_{21}^{S,k}\right]^{-1} & -\mathbf{S}_{22}^{S,k}\left[\mathbf{S}_{21}^{S,k}\right]^{-1} \\ \hline \left[\mathbf{S}_{21}^{S,k}\right]^{-1}\mathbf{S}_{11}^{S,k} & \mathbf{S}_{12}^{S,k} - \mathbf{S}_{11}^{S,k}\left[\mathbf{S}_{21}^{S,k}\right]^{-1}\mathbf{S}_{22}^{S,k} \end{array}\right], \end{aligned} \tag{10}$$

where $\mathbf{T}_{11}^{T,k}$, $\mathbf{T}_{12}^{T,k}$, $\mathbf{T}_{21}^{T,k}$, $\mathbf{T}_{22}^{T,k}$ are the $n \times n$ matrix elements of the $\mathbf{T}^{T,k}$ as determined by (9) and $\mathbf{T}_{11}^{S,k}$, $\mathbf{T}_{12}^{S,k}$, $\mathbf{T}_{21}^{S,k}$, $\mathbf{T}_{22}^{S,k}$ are the $n \times n$ matrix elements of the $\mathbf{T}^{S,k}$ as evaluated from (10). Taking into consideration (9) and (10), the $2n\times2n$ chain scattering matrix of a "branch" module, $\mathbf{T}^{k}$, is determined in the appropriate cascade rule order through the following multiplication rule [27, 28, 71, 72]:

$$\begin{aligned} \mathbf{T}^{k} &= \mathbf{T}^{T,k} \cdot \mathbf{T}^{S,k} \\ &= \left[\begin{array}{c|c} \mathbf{T}_{11}^{T,k}\mathbf{T}_{11}^{S,k} + \mathbf{T}_{12}^{T,k}\mathbf{T}_{21}^{S,k} & \mathbf{T}_{11}^{T,k}\mathbf{T}_{12}^{S,k} + \mathbf{T}_{12}^{T,k}\mathbf{T}_{22}^{S,k} \\ \hline \mathbf{T}_{21}^{T,k}\mathbf{T}_{11}^{S,k} + \mathbf{T}_{22}^{T,k}\mathbf{T}_{21}^{S,k} & \mathbf{T}_{21}^{T,k}\mathbf{T}_{12}^{S,k} + \mathbf{T}_{22}^{T,k}\mathbf{T}_{22}^{S,k} \end{array}\right]. \end{aligned} \tag{11}$$

The last module of the BPL connection is the "load" module. Similarly to "transmission" submodule characteristics of (9), the $2n \times 2n$ chain scattering matrix of the "load" module is given by

$$\mathbf{T}^{N+1} = \left[\begin{array}{c|c} \left[\mathbf{E}^{T,N+1}\right]^{-1} & \mathbf{0}_{n\times n} \\ \hline \mathbf{0}_{n\times n} & \mathbf{E}^{T,N+1} \end{array}\right]. \tag{12}$$

Having determined the chain scattering matrices of the various network modules encountered along the end-to-end connection, as it has already been detailed in [71, 72], the $2n \times 2n$ overall end-to-end chain scattering matrix is evaluated through the multiplication rule of (11) from

$$\mathbf{T}^{\text{overall}} = \left[\begin{array}{c|c} \mathbf{T}_{11}^{\text{overall}} & \mathbf{T}_{12}^{\text{overall}} \\ \hline \mathbf{T}_{21}^{\text{overall}} & \mathbf{T}_{22}^{\text{overall}} \end{array}\right] = \prod_{k=1}^{N+1} \mathbf{T}^{k}, \tag{13}$$

and the $2n \times 2n$ overall end-to-end scattering matrix is obtained from

$$\mathbf{S}^{\text{overall}} = \left[\begin{array}{c|c} \mathbf{S}_{11}^{\text{overall}} & \mathbf{S}_{12}^{\text{overall}} \\ \hline \mathbf{S}_{21}^{\text{overall}} & \mathbf{S}_{22}^{\text{overall}} \end{array}\right] = \left[\begin{array}{c|c} \mathbf{T}_{21}^{\text{overall}}\left[\mathbf{T}_{11}^{\text{overall}}\right]^{-1} & \mathbf{T}_{22}^{\text{overall}} - \mathbf{T}_{21}^{\text{overall}}\left[\mathbf{T}_{12}^{\text{overall}}\right]^{-1}\mathbf{T}_{11}^{\text{overall}} \\ \hline \left[\mathbf{T}_{11}^{\text{overall}}\right]^{-1} & -\left[\mathbf{T}_{12}^{\text{overall}}\right]^{-1}\mathbf{T}_{11}^{\text{overall}} \end{array}\right], \tag{14}$$

where $\mathbf{T}_{11}^{\text{overall}}$, $\mathbf{T}_{12}^{\text{overall}}$, $\mathbf{T}_{21}^{\text{overall}}$, $\mathbf{T}_{22}^{\text{overall}}$ are the $n \times n$ matrix elements of the $\mathbf{T}^{\text{overall}}$ as evaluated from (13) and $\mathbf{S}_{11}^{\text{overall}}$, $\mathbf{S}_{12}^{\text{overall}}$, $\mathbf{S}_{21}^{\text{overall}}$, $\mathbf{S}_{22}^{\text{overall}}$ are the $n \times n$ elements of the $\mathbf{S}^{\text{overall}}$ matrix as defined from (14).

Combining (4) and (14), the $n \times n$ modal transfer function matrix is given by the $\mathbf{S}_{21}^{\text{overall}}$ element of the $\mathbf{S}^{\text{overall}}$ matrix, that is,

$$\mathbf{H}^{m}\{\cdot\} = \mathbf{S}_{21}^{\text{overall}} = \left[\mathbf{T}_{11}^{\text{overall}}\right]^{-1}. \tag{15}$$

The proposed TM2 method is extremely flexible since it is also able to calculate modal transfer functions associated with any type of BPL distribution network including various types of overhead and underground LV/BPL and MV/BPL configurations, any type of interconnection at the branches, and any type of branch termination. This permits the direct application of TM2 method in contrast with legacy SM and TM methods where the assumption of specific transmission assumptions were necessary, thus limiting their general application [1, 8–11, 22, 28, 73]. Finally, contrary to SM and TM methods, the problem of mode mixture now can be fully investigated through the definition of the modal XC transfer functions, as given in (15).

## 4. Statistical Performance Metrics of the Modal Channels

Extending the statistical performance metrics of overhead HV/BPL coupling scheme channels presented in [19], based on the end-to-end modal transfer functions of the independent modal BPL transmission channels, as given by (15), several useful modal metrics are first presented concerning the statistical properties of the $n \times n$ BPL modal channels existing in overhead and underground LV and MV configurations, as follows.

(a) *The modal discrete impulse response.* Once the end-to-end modal transfer function is known from (15), modal discrete impulse response $h_{i,j,p}^{m} = h_{i,j}^{m}(t = pT_s)$, $p = 0,\ldots,J-1$, $i,j = 1,\ldots,n$ is obtained as the power of two $J$-point inverse discrete Fourier

transform (IDFT) of the discrete end-to-end modal transfer function:

$$H_{i,j,q}^{m} = \begin{Bmatrix} \left|H_{i,j,q}^{m}\right| e^{j\varphi_{i,j,q}^{m}}, & q = 0,\ldots,K-1 \\ 0, & q = K,\ldots,J-1 \end{Bmatrix} = \begin{Bmatrix} H_{i,j}^{m}(f = qf_s), & q = 0,\ldots,K-1 \\ 0, & q = K,\ldots,J-1 \end{Bmatrix}, \quad i,j = 1,\ldots,n, \tag{16}$$

where $j$ is the imaginary unit, $F_s = 1/T_s$ is the Nyquist sampling rate, $f_s$ is the flat-fading subchannel frequency span, $K \le J/2$ is the number of subchannels in the BPL signal frequency range of interest, and $|H_{i,j,q}^{m}|$ and $\phi_{i,j,q}^{m}$ are the amplitude response and the phase response of the discrete end-to-end modal transfer function, respectively [19, 33–35].

(b) *The average end-to-end modal channel gain*. As the BPL channel is frequency selective, the average end-to-end modal channel gain can be calculated by averaging over frequency

$$\overline{\left|H_{i,j}^{m}\right|^2} = \frac{1}{J}\sum_{q=0}^{J-1}\left|H_{i,j,q}^{m}\right|^2 = \sum_{q=0}^{J-1}\left|h_{i,j,q}^{m}\right|^2, \quad i,j = 1,\ldots,n, \tag{17}$$

where $\overline{|H_{i,j}^{m}|^2}$, $i, j = 1,\ldots,n$ is the average end-to-end modal channel gain. The lognormality (normality) of the average end-to-end modal channel gain may be justified by the multipath nature of BPL signal propagation and the TL modeling using on cascaded two-port network modules [19, 33–35, 38–41].

(c) *The modal RMS-DS*. It is a measure of the multipath richness of a BPL modal channel. The modal RMS-DS is determined from [19, 33–35, 38–41]:

$$\sigma_{\tau,i,j}^{m} = T_s\sqrt{\mu_{0,i,j}^{m,(2)} - \left(\mu_{0,i,j}^{m}\right)^2}, \quad i,j = 1,\ldots,n, \tag{18}$$

where

$$\mu_{0,i,j}^{m} = \frac{\sum_{p=0}^{J-1} p\left|h_{i,j,p}^{m}\right|^2}{\sum_{p=0}^{J-1}\left|h_{i,j,p}^{m}\right|^2}, \quad i,j = 1,\ldots,n,$$
$$\mu_{0,i,j}^{m,(2)} = \frac{\sum_{p=0}^{J-1} p^2\left|h_{i,j,p}^{m}\right|^2}{\sum_{p=0}^{J-1}\left|h_{i,j,p}^{m}\right|^2}, \quad i,j = 1,\ldots,n. \tag{19}$$

(d) *The relationship between end-to-end modal channel attenuation and modal RMS-DS*. Recently, several statistical channel models have investigated the correlation between end-to-end BPL channel attenuation and RMS-DS which appears to be a universal property of wireline channels (e.g., overhead HV/BPL, DSL, coaxial, and phone link channels) [19, 33–41]. In this paper, the already proposed approaches for coupling scheme channels are extended so as to describe modal channels, say these approximations aim at identifying the distribution of the end-to-end modal channel attenuation and modal RMS-DS. Their main advantage is that they summarize statistical results carried out on a variety of BPL system data sets proposing suitable trend lines for overhead and underground LV/BPL and MV/BPL modal channels of the following form:

$$\left(\sigma_{\tau,i,j}^{m}\right)_{\mu s} = v_{i,j}\cdot\left(\overline{A_{i,j}^{m}}\right)_{\mathrm{dB}} + w_{i,j}, \quad i,j = 1,\ldots,n, \tag{20}$$

where

$$\left(\overline{A_{i,j}^{m}}\right)_{\mathrm{dB}} = -\left(\overline{\left|H_{i,j}^{m}\right|^2}\right)_{\mathrm{dB}}, \quad i,j = 1,\ldots,n \tag{21}$$

is the average end-to-end channel attenuation in dB, $(\sigma_{\tau,i,j}^{m})_{\mu s}$ is the RMS-DS in $\mu s$, and $(\overline{|H_{i,j}^{m}|^2})_{\mathrm{dB}}$ is the average end-to-end channel gain in dB of the BPL modal channel examined. Parameters $v_{i,j}$ and $w_{i,j}$ constitute the robust regression parameters and are calculated using appropriate robust regression techniques depending on the modal channel considered and the technique adopted.

(e) *The attenuation exceedance probability*. It is the probability that the end-to-end modal channel attenuation $A_{i,j}^{m}$, $i, j = 1,\ldots,n$ exceeds a certain level. The distribution of the attenuation exceedance probability may be determined for any overhead or underground LV/BPL or MV/BPL channel. It provides a qualitative macroscopic estimate of how steep is the end-to-end attenuation of BPL channels and may help to determine: (i) the positions where the installation of signal repeaters is necessary in SG networks; (ii) the thresholds related to the application of orthogonal frequency-division multiplexing (OFDM) systems, discrete multitone modulation (DMT) systems, and of various resource allocation schemes [8, 9, 11, 17, 19, 74–76].

## 5. Numerical Results and Discussion

The simulations of various types of overhead and underground LV/BPL and MV/BPL transmission modal channels aim at investigating (a) their broadband transmission characteristics; (b) how their spectral behavior is affected by several factors, such as the type and the topology of the distribution power grid; (c) statistical remarks obtained on the basis of simulated and measured BPL topologies.

For the numerical computations, the overhead and underground LV and MV distribution line configurations depicted in Figures 1(a)–1(d), respectively, have been considered. As already mentioned in Section 2 and analyzed in Section 3, since the modal channels supported by the overhead and underground LV/BPL and MV/BPL configurations may be examined separately, it is assumed for simplicity that the BPL signal is injected directly into the modal channels [1, 8–11, 19, 22–24, 26, 27, 30, 31, 42, 73]; thus, the complicated

modal analysis of [30, 31], briefly described in Sections 2 and 3, is avoided. In addition, since the mode mixing is not among the scopes and contributions of this paper, the following analysis is concentrated only on the investigation of modal CC transfer functions rather than XC ones.

As it concerns the system specifications, the sampling rate and flat-fading subchannel frequency spacing are assumed $F_s = 200\,\text{MHz}$ and $f_s = 0.2\,\text{MHz}$, respectively. Thus, the number of subchannels $K$ in the BPL signal frequency range of interest and the $J$-point IDFT are assumed equal to 496 and 1024, respectively.

As usually done to simplify the analysis [1, 8–11, 19–21, 42, 48, 54, 57, 62, 68], only one mode for each BPL system will be examined, hereafter. This assumption does not affect the generality of the analysis concerning the transmission characteristics of the examined BPL systems in the range from 1 MHz to 100 MHz and is adopted for the sake of terseness, economy, and simplicity. Hence, the transmission characteristics of only one mode for each BPL system, say that of $\text{DM}_1$, will be examined, hereafter. Consequently, only the CC transmission characteristics of $\text{DM}_1^{\text{OV,LV}}$, $\text{DM}_1^{\text{OV,MV}}$, $\text{DM}_1^{\text{UN,LV}}$, and $\text{DM}_1^{\text{UN,MV}}$, for overhead LV/BPL, overhead MV/BPL, underground LV/BPL, and underground MV/BPL systems, respectively, will be examined in the rest of the paper.

The simple BPL topology of Figure 3(a), having $N$ branches, has been considered. In order to validate the accuracy of TM2 method and simplify the following analysis without affecting its generality, the branching TLs are assumed identical to the distribution TLs and the interconnections between the distribution and branch conductors are fully activated. With reference to Figure 3(c), the transmitting and the receiving ends are assumed matched to the characteristic impedance of the mode considered, whereas the branch terminations $\mathbf{Z}_{bk}$, $k = 1,\ldots,N$ are assumed open circuit, that is, $\mathbf{K}_{bk} = \mathbf{I}_{n^{bk}}$, $k = 1,2,\ldots,N$ where $\mathbf{I}_{n^{bk}}$ is the $n^{bk} \times n^{bk}$ identity matrix—[1, 4, 8–11, 19–22, 42].

In urban areas, about 45%–75% of the underground grids exhibit path lengths shorter than 200 m and only 1%–9% longer than 500 m. The latter case constitutes the worst-case scenario with regard to underground BPL transmission [4, 5, 55]. Hence, path lengths of the order of 200 m to 250 m are encountered in underground BPL transmission. These path lengths are quite shorter compared to the overhead BPL case where path lengths up to 1000 m may be encountered [1, 4, 5, 9, 11–13, 22, 23, 42, 44, 48, 55, 64, 77, 78].

With reference to Figure 3(c), five indicative overhead topologies, which are common for both overhead LV/BPL and MV/BPL systems, concerning end-to-end connections of average lengths equal to 1000 m have been examined, as follows.

(1) A typical overhead urban topology (overhead urban case A) with $N = 3$ branches ($L_1 = 500\,\text{m}$, $L_2 = 200\,\text{m}$, $L_3 = 100\,\text{m}$, $L_4 = 200\,\text{m}$, $L_{b1} = 8\,\text{m}$, $L_{b2} = 13\,\text{m}$, $L_{b3} = 10\,\text{m}$).

(2) An aggravated overhead urban topology (overhead urban case B) with $N = 5$ branches ($L_1 = 200\,\text{m}$, $L_2 = 50\,\text{m}$, $L_3 = 100\,\text{m}$, $L_4 = 200\,\text{m}$, $L_5 = 300\,\text{m}$, $L_6 = 150\,\text{m}$, $L_{b1} = 12\,\text{m}$, $L_{b2} = 5\,\text{m}$, $L_{b3} = 28\,\text{m}$, $L_{b4} = 41\,\text{m}$, $L_{b5} = 17\,\text{m}$).

(3) A typical overhead suburban topology (overhead suburban case) with $N = 2$ branches ($L_1 = 500\,\text{m}$, $L_2 = 400\,\text{m}$, $L_3 = 100\,\text{m}$, $L_{b1} = 50\,\text{m}$, $L_{b2} = 10\,\text{m}$).

(4) A typical overhead rural topology (overhead rural case) with only $N = 1$ branch ($L_1 = 600\,\text{m}$, $L_2 = 400\,\text{m}$, $L_{b1} = 300\,\text{m}$).

(5) The overhead "LOS" transmission along the same end-to-end distance $L = L_1 + \cdots + L_{N+1} = 1000\,\text{m}$ when no branches are encountered.

The respective indicative underground topologies, which are common for both underground LV/BPL and MV/BPL systems, concern 200 m long end-to-end connections. These topologies are as follows.

(1) A typical underground urban topology (underground urban case A) with $N = 3$ branches ($L_1 = 70\,\text{m}$, $L_2 = 55\,\text{m}$, $L_3 = 45\,\text{m}$, $L_4 = 30\,\text{m}$, $L_{b1} = 12\,\text{m}$, $L_{b2} = 7\,\text{m}$, $L_{b3} = 21\,\text{m}$).

(2) An aggravated underground urban topology (underground urban case B) with $N = 5$ branches ($L_1 = 40\,\text{m}$, $L_2 = 10\,\text{m}$, $L_3 = 20\,\text{m}$, $L_4 = 40\,\text{m}$, $L_5 = 60\,\text{m}$, $L_6 = 30\,\text{m}$, $L_{b1} = 22\,\text{m}$, $L_{b2} = 12\,\text{m}$, $L_{b3} = 8\,\text{m}$, $L_{b4} = 2\,\text{m}$, $L_{b5} = 17\,\text{m}$).

(3) A typical underground suburban topology (underground suburban case) with $N = 2$ branches ($L_1 = 50\,\text{m}$, $L_2 = 100\,\text{m}$, $L_3 = 50\,\text{m}$, $L_{b1} = 60\,\text{m}$, $L_{b2} = 30\,\text{m}$).

(4) A typical underground rural topology (rural case) with only $N = 1$ branch ($L_1 = 50\,\text{m}$, $L_2 = 150\,\text{m}$, $L_{b1} = 100\,\text{m}$).

(5) The underground "LOS" transmission along the same end-to-end distance $L = L_1 + \cdots + L_{N+1} = 200\,\text{m}$ when no branches are encountered.

*5.1. TM2 Method Verification and Effect of Grid Topology on Overhead and Underground LV/BPL and MV/BPL Transmission.* To compare the proposed TM2 method with other established methods [11, 16, 19–21, 32, 79] and simultaneously examine the end-to-end modal channel attenuation behavior for different LV/BPL and MV/BPL types and topologies, in Figures 4(a)–4(e), the end-to-end channel attenuation from A to B for the propagation of $\text{DM}_1$ is plotted with respect to frequency for the aforementioned five indicative overhead LV topologies, respectively, applying the proposed TM2 method, the TM method [11, 19–21], and the multipath echo-based (MEB) method [6, 16, 79]. In Figures 4(f)–4(t), similar plots are drawn in the case of overhead MV, underground LV, and underground MV indicative topologies, respectively. Observations based on Figures 4(a)–4(t) were made as follows.

(i) As it concerns the validity of TM2 method, it is observed that the three methods coincide in all

the BPL types and topologies examined yielding excellent results of convergence regardless of the overhead/underground power grid type and topology. Moreover, since in a realistic BPL distribution network, due to reflections and multipath propagation caused by branches, spectral notches are observed in the end-to-end modal channel attenuation, the accurate description of the number and the behavior of these spectral notches consist a crucial and defining element in order to obtain a representative image of their real behavior. Actually, The TM2 method describes the spectral notches accurately either in depth or in spectral extent in any multipath environment. Thus, the TM2 method offers an accurate representation of the attenuation discontinuities caused by branching. It is also easily adapted to various network topologies resulting from various kinds of branches or transformers [8, 19, 55, 64, 77, 78]. Due to the unique combination of generality and modular simplicity, the TM2 method will be adopted in the following simulations concerning the behavior of overhead and underground LV/BPL and MV/BPL modal channels.

(ii) In a realistic BPL network, the spectral behavior of the end-to-end channel attenuation depends drastically on the frequency, the type of grid, the physical properties of the cables used, the end-to-end—"LOS"—distance, and the number, the electrical length, and the terminations of the branches encountered along the end-to-end BPL signal transmission path [6, 8, 9, 11, 16, 19, 55, 64, 68, 77]. As it has been pointed out from the above figures, due to reflections and multipath propagation caused by branches, spectral notches are observed in the end-to-end channel attenuation. The number and the behavior of these spectral notches significantly depend on the number of branches encountered along the end-to-end transmission path as well as on the branch electrical length. These spectral notches are superimposed on the exponential "LOS" attenuation [8, 19, 55, 64, 77, 78].

In Figures 5(a) and 5(b), the attenuation exceedance probability of $DM_1$ is plotted versus end-to-end channel attenuation for the aforementioned indicative LV and MV topologies, respectively. As readily verified observing the respective attenuation distributions, the attenuation exhibited by underground channels is dramatically worse than the attenuation of overhead ones. This explains why in most underground channels distance rather than multipath is identified as the dominant factor affecting signal transmission. The opposite is observed in overhead channels, where the effect of multipath is significantly more severe and is recognized as the primary attenuation factor. Therefore, in urban and suburban environments denser BPL networks are preferable [4, 5, 8–11, 55].

Based on the picture of the spectral behavior obtained from Figures 4(a)–4(t) and Figures 5(a) and 5(b), as it has already been mentioned in the case of overhead HV/BPL systems, the taxonomy of BPL distribution grids remains the same; the BPL modal channels may be classified into the following three channel classes [8–11, 19, 41, 75, 80].

(i) "LOS" *channels*, representing end-to-end transmission when no intermediate branches exist. No spectral notches are observed. This case corresponds to the best possible BPL transmission conditions, encountered sometimes in rural or suburban and rarely in urban areas.

(ii) *Good channels*, when a small number of relatively long branches are encountered along the end-to-end connection. Shallow spectral notches are observed. BPL transmission in rural, suburban, and several urban areas belongs to this channel class.

(iii) *Bad channels*, when the number of branches is large and their electrical length is small. Deep spectral notches are observed. BPL transmission in many urban areas belongs to this channel class.

The spectral behavior of the above BPL modal channel classes critically affects the transmission characteristics of BPL modal channels.

*5.2. On the Statistical Relationship between End-to-End Modal Channel Attenuation and Modal RMS-DS.* Based on the statistical performance metrics presented in Section 4 and the notion already acquired from overhead HV/BPL coupling scheme channels in [19], a physically meaningful statistical characterization of the BPL modal channels is obtained permitting important properties of the overhead and underground LV/BPL and MV/BPL to come to light. Table 1 summarizes the metrics of average end-to-end modal channel attenuation and modal RMS-DS for the aforementioned indicative overhead and underground LV/BPL and MV/BPL topologies for the propagation of $DM_1$.

Similarly to [19], the spectral behavior of overhead and underground LV/BPL and MV/BPL modal channels is reflected on the corresponding statistical performance metrics. Indeed, though determined for 1000 m long connections, compared to the 200 m long connections of the underground cases, the metric of average end-to-end modal channel attenuation of overhead transmission is significantly better than the underground one. Furthermore, an indicative picture of the above channel classification can be obtained studying the metric of modal RMS-DS. Since, in bad channel class, superimposed multipath critically affects signal transmission, bad channel class—primarily urban case B and secondarily urban case A—tends to exhibit higher values of modal RMS-DS in comparison with the good channel class, either suburban or rural cases. "LOS" channels are characterized by the best possible modal RMS-DS values, as these channels represent end-to-end transmission when no multipath exists.

Recently, several statistical approaches investigating the relationship of end-to-end attenuation and RMS-DS have been proposed [19, 33–41, 55]. Various measurements for different BPL topologies have been also performed in the

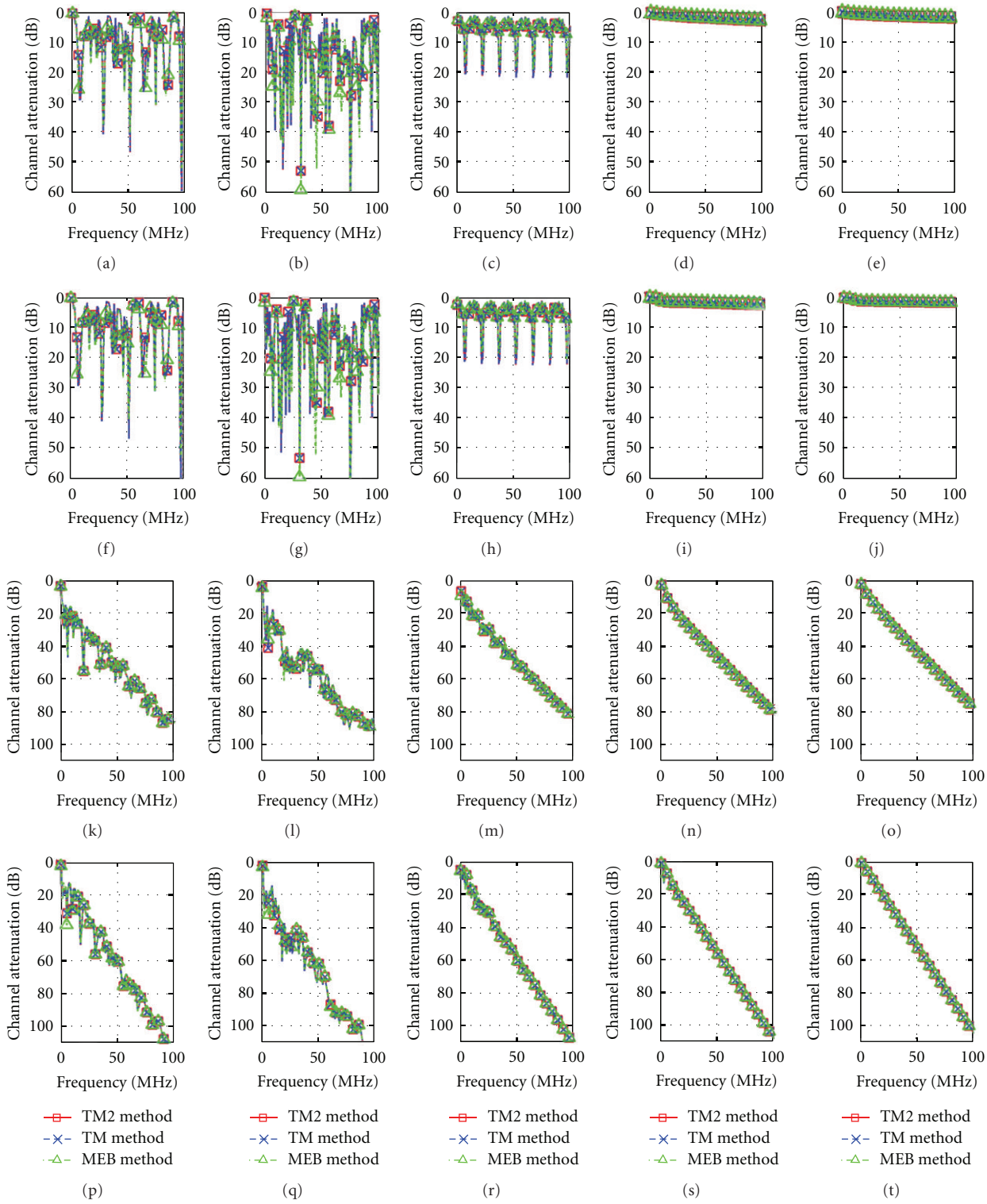


Figure 4: Application of the coinciding proposed TM2 method, TM method, and MEB method to determine the end-to-end channel attenuation for the propagation of $DM_1$ versus frequency for different overhead and underground LV/BPL and MV/BPL types and topologies (the subchannel frequency spacing is equal to 1 MHz). (a) Urban case A/overhead LV. (b) Urban case B/overhead LV. (c) Suburban case/overhead LV. (d) Rural case/overhead LV. (e) "LOS" case/overhead LV. (f) Urban case A/overhead MV. (g) Urban case B/overhead MV. (h) Suburban case/overhead MV. (i) Rural case/overhead MV. (j) "LOS" case/overhead MV. (k) Urban case A/underground LV. (l) Urban case B/underground LV. (m) Suburban case/underground LV. (n) Rural case/underground LV. (o) "LOS" case/underground LV. (p) Urban case A/underground MV. (q) Urban case B/overhead MV. (r) Suburban case/overhead MV. (s) Rural case/overhead MV. (t) "LOS" case/underground MV.

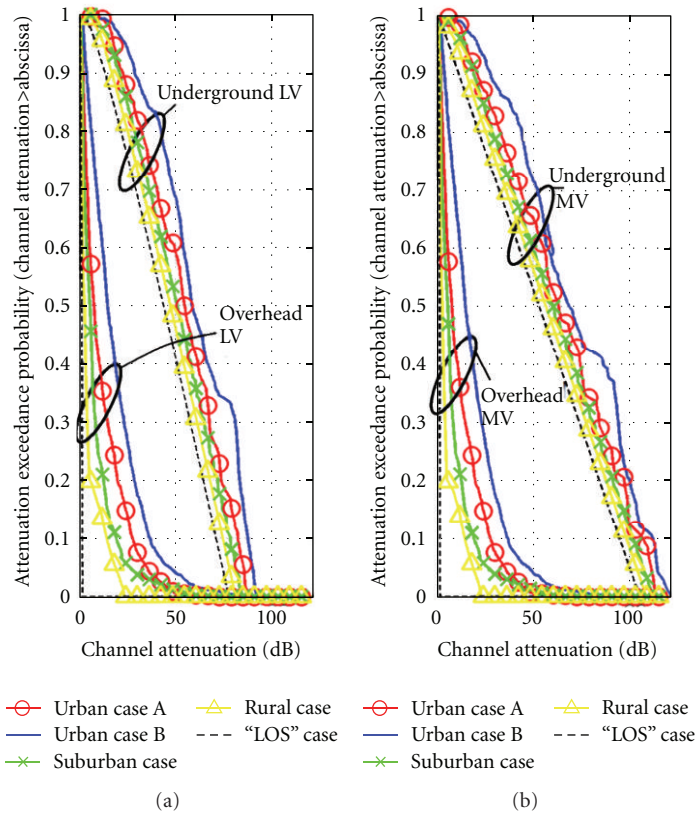


FIGURE 5: Attenuation exceedance probability of $DM_1$ versus frequency for urban case A, urban case B, suburban case, rural case, and "LOS" transmission case. (a) Overhead and underground LV. (b) Overhead and underground MV.

frequency range from 1 MHz to 100 MHz focusing on the evaluation of distribution function between average end-to-end channel attenuation and RMS-DS. These measurements may be classified into the following set:

(i) field trial measurements in real in-home LV/BPL suburban and urban networks [36, 37];

(ii) field trial measurements in underground MV/BPL power network [33–35].

The correlation between average end-to-end channel attenuation and RMS-DS can be easily verified observing the scatter plot presented in Figure 6 where the above set of measurements and the set of numerical results of $DM_1$ for the aforementioned indicative overhead and underground LV/BPL and MV/BPL topologies, presented analytically in Table 1 and denoted as overhead LV/BPL power networks, overhead MV/BPL power networks, underground LV/BPL power networks, and underground MV/BPL power networks, are plotted. In the same figure, regression lines, as given by (20), are also plotted, namely, (i) GAL approach, as proposed in [33–35], with robust regression parameters assumed $v = 0.0075\,\mu$s/dB and $w = 0.183\,\mu$s; (ii) TON approach, as given by [39], with robust regression parameters $v$ and $w$ assumed equal to 0.0197 $\mu$s/dB and 0 $\mu$s, respectively; (iii) the proposed UNI[1] approach, as defined in [19], with regression parameters $v = 0.0129\,\mu$s/dB and $w = 0.2472\,\mu$s.

From Figure 6, the following should be mentioned.

(i) The field measurements, the numerical results, and the approximation curves exhibit a positive slope clearly indicating that average end-to-end modal channel attenuation and modal RMS-DS are also positively correlated lognormal random variables of overhead and underground LV/BPL and MV/BPL systems in accordance with coupling scheme channel correlation of [19]. The detailed theoretical analysis and the respective statistical tests are presented in [33–35].

(ii) The proposed UNI[1] trend line suggests a unified regression line that describes the correlation between channel attenuation and RMS-DS both in transmission and in distribution power grids regardless of the type of channel described—either coupling scheme or modal channels—and the system specifications. Hence, UNI[1] approach offers a useful tool towards BPL/SG systems coexistence as it can be used to estimate the maximum data rate of BPL power grids being supported without the use of an equalizer [19].

(iii) Depending on the system specifications, a rule of thumb holds that the position of the BPL channel markers in the scatter plot in relation with the appropriate approximation curve defines the BPL class of the channel. Therefore, markers located significantly above the curve result in an above average RMS-DS

Table 1: Performance Statistical Metrics of Section 4.

| | Average end-to-end channel attenuation of $DM_1$ (dB) | | | | RMS-DS of $DM_1$ ($\mu$s) | | | |
|---|---|---|---|---|---|---|---|---|
| | Overhead | | Underground | | Overhead | | Underground | |
| | LV | MV | LV | MV | LV | MV | LV | MV |
| Urban case A | 9.07 | 9.18 | 26.91 | 24.92 | 0.53 | 0.76 | 0.62 | 0.64 |
| Urban case B | 12.25 | 12.39 | 28.56 | 26.62 | 0.94 | 1.00 | 0.74 | 0.77 |
| Suburban case | 7.78 | 7.92 | 25.78 | 23.21 | 0.39 | 0.59 | 0.48 | 0.55 |
| Rural case | 6.20 | 6.35 | 23.00 | 20.68 | 1.36 | 1.35 | 0.51 | 0.58 |
| "LOS" case | 4.22 | 4.34 | 19.98 | 17.90 | 0.07 | 0.35 | 0.31 | 0.28 |

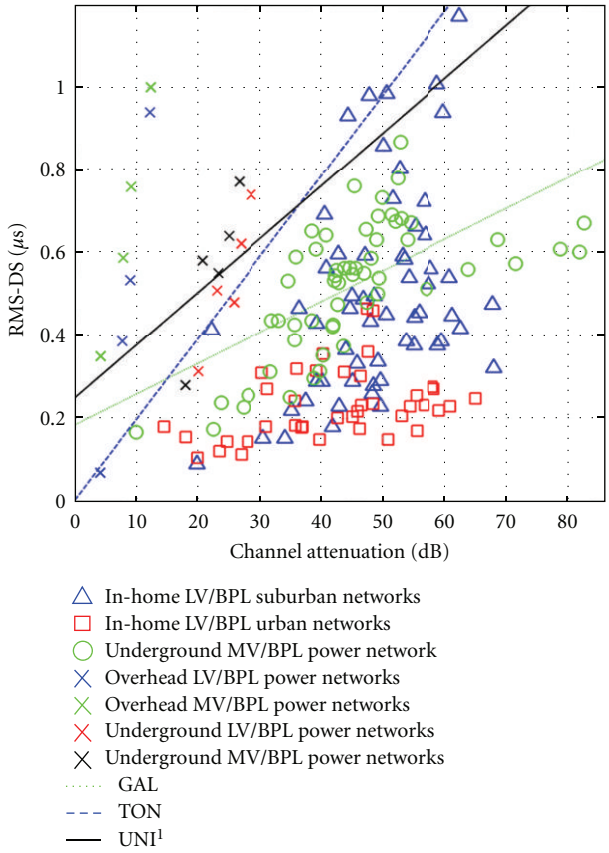


Figure 6: Scatter plot of RMS-DS versus average end-to-end channel attenuation for measured channels (in-home LV/BPL suburban networks, in-home LV/BPL urban networks, and underground MV/BPL power network), simulated channels (overhead LV/BPL power networks, overhead MV/BPL power networks, underground LV/BPL power networks, and underground MV/BPL power networks for the propagation of DM1), and trend line curves (GAL, TON, and UNI1 approaches).

for given average end-to-end channel attenuation. In the case of the above examined overhead and underground LV/BPL and MV/BPL systems compared to UNI[1] curve, the above average RMS-DS channels are the bad class ones, for example, urban case B. The opposite is observed in "LOS" and good channel cases where the channel markers of these cases are located either below or near to the UNI[1] curve, for example, "LOS" and rural cases, respectively.

(iv) On the basis of the confirmed correlation, statistical channel models may be defined. These models can generate random overhead and underground LV and MV topologies by setting the topology parameters on the basis of channel class characteristics. Consequently, these models confer a stochastic aspect to the deterministic channel class design [33–41].

(v) The deterministic BPL channel models in combination with the newly born statistical BPL channel models will aid in gaining a necessary tool when LV/BPL and MV/BPL systems need to coexist in the SG field.

*5.3. Comparison and Integration between Overhead and Underground LV/BPL and MV/BPL Systems.* Concluding the analysis of overhead and underground LV/BPL and MV/BPL transmission, the following distinct characteristics should be marked out.

(1) Based on the well-established hybrid model of [8–11, 19–21] and the generic multidimensional network analysis tool presented in [22–24], a novel multidimensional chain scattering matrix method (TM2 method) has successfully been applied in overhead and underground LV/BPL and MV/BPL systems. First of all, TM2 method is well validated against other theoretically and experimentally proven models, such as MEB and TM methods. Moreover, TM2 method is able to calculate modal transfer functions associated with very elaborate networks including various types of overhead and underground LV/BPL and MV/BPL configurations, any type of interconnection at the branches, and any type of branch termination without imposing special simplifying transmission assumptions. Finally, TM2 method provides significant help regarding mode mixture issues via the definition of modal XC transfer functions, which describe the crosstalk couplings among the modes supported.

(2) As a broadband communications channel, the overhead and underground LV/BPL and MV/BPL distribution power grids suffer from multipath and "LOS" attenuation which adversely affect the BPL system design and the SG application performance.

Besides the BPL power distribution grid considered, the end-to-end attenuation in BPL modal channels along the end-to-end transmission path depends on the frequency, the mode considered, the physical properties of the MTL configurations used, end-to-end—"LOS"—distance and the number, the electrical length, and the terminations of the various branches encountered along the end-to-end BPL signal propagation [9–11, 20, 21, 23, 25, 55, 64, 77, 78]. As it has already been reported in [19, 20], the same factors also influence the spectral behavior of overhead HV/BPL transmission power grids.

(3) The taxonomy of BPL modal channels into three classes depending on the behavior of spectral notches is still maintained in the case of BPL distribution grids, namely, "LOS" channels, good channels and bad channels. BPL transmission in the majority of suburban and rural areas and in several urban areas is classified into the good channel class [8, 9, 11, 19–21, 25, 38, 41, 80].

(4) Since "LOS" attenuation is dominant in underground BPL transmission, multipath affects underground transmission considerably less compared to overhead BPL transmission. Therefore, BPL signal transmission via the underground grid exhibits a lowpass behavior which limits the BPL bandwidth exploitation potential up to a certain frequency [6–11, 15].

(5) In BPL channels, it has been verified that channel attenuation and RMS-DS are (positively) correlated lognormal random variables. This fundamental property of several wireline systems (e.g., DSL, coaxial, and phone links) has been validated also in the BPL system case either in modal or in coupling scheme channels [19–21, 33–41]. Since this inherent statistical characteristic has also been validated in the case of overhead HV/BPL transmission power grids [19], suitable unified approximations can be proposed, such as GAL [33–35], TON [39], and UNI[1] [19] regression trend lines, that commonly describe either distribution or transmission BPL power grids regardless of the type of channel described. This introduction of unified tools for the common handling of BPL transmission and distribution networks is to be seen as strong interoperability guarantee in a SG landscape.

(6) In the SG landscape, overhead and underground LV/BPL and MV/BPL systems need to work in a compatible way (intraoperate) before BPL technology interoperates with other broadband technologies, such as wired (e.g., fiber and DSL) and wireless (e.g., WiFi and WiMax). A prerequisite step towards SG technology integration requires compatible frequencies, equipment and signaling, adequate injected power spectral density (IPSD) levels, area coverage, and scalable capacity among BPL systems, taking the specific features of LV/BPL and MV/BPL transmission into account [8–11, 17, 19–21, 25, 33, 75, 81].

## 6. Conclusions

This paper has focused on the broadband modal signal transmission characteristics and the modal statistical performance metrics of overhead and underground LV and MV distribution power grids based on a new exact multidimensional chain scattering matrix method (TM2 method). The TM2 method which may be combined with an extended statistical metric framework offers a valuable tool towards the integrated transmission and distribution BPL network design.

TM2 method has revealed that the broadband modal signal transmission capability of overhead and underground LV/BPL and MV/BPL networks depends on the frequency, the type of the power grid, the mode considered, physical properties of the MTL configuration used, the end-to-end—"LOS"—distance, and the number, the electrical length, and the terminations of the branches along the end-to-end BPL signal propagation.

Based on the modal statistical performance metrics of overhead and underground LV/BPL and MV/BPL distribution networks, a fundamental property of several wireline and other BPL channels, that is the positive correlation between end-to-end channel attenuation and RMS-DS, has also been validated in the case of BPL systems against relevant sets of field measurements, numerical results, and recently proposed statistical channel models for BPL systems. Based on these inherent attributes of: (i) either distribution or transmission BPL systems and (ii) either modal or coupling scheme channels, a new regression trend line suitable for the common handling of BPL systems has been applied.

The transmission characteristics, the statistical performance metrics, and the insertion of unified tools determine the deployment of OFDM/DMT systems, the unified design/operation of BPL systems, the performance of various SG applications across the entire transmission and distribution grid, and the BPL system intraoperability/interoperability in a heterogeneous set of networking technologies such as the oncoming SG network.

## References

[1] A. G. Lazaropoulos and P. G. Cottis, "Transmission characteristics of overhead medium-voltage power-line communication channels," *IEEE Transactions on Power Delivery*, vol. 24, no. 3, pp. 1164–1173, 2009.

[2] G. Jee, R. D. Rao, and Y. Cern, "Demonstration of the technical viability of PLC systems on medium- and low-voltage lines in the United States," *IEEE Communications Magazine*, vol. 41, no. 5, pp. 108–112, 2003.

[3] F. J. Cañete, J. A. Cortés, L. Díez, and J. T. Entrambasaguas, "A channel model proposal for indoor power line communications," *IEEE Communications Magazine*, vol. 49, no. 12, pp. 166–174, 2011.

[4] OPERA1, D44: Report presenting the architecture of plc system, the electricity network topologies, the operating modes and the equipment over which PLC access system will be installed, IST Integr. Project No 507667, 2005.

[5] DLC+VIT4IP, D1.2: Overall system architecture design DLC system architecture. FP7 Integrated Project No 247750, 2010,

http://www.dlc-vit4ip.org/wb/media/Downloads/D1.2%20system%20architecture%20design.pdf.

[6] K. Dostert, *Powerline Communications*, Prentice-Hall, Upper Saddle River, NJ, USA, 2001.

[7] M. Gebhardt, F. Weinmann, and K. Dostert, "Physical and regulatory constraints for communication over the power supply grid," *IEEE Communications Magazine*, vol. 41, no. 5, pp. 84–90, 2003.

[8] P. Amirshahi and M. Kavehrad, "High-frequency characteristics of overhead multiconductor power lines for broadband communications," *IEEE Journal on Selected Areas in Communications*, vol. 24, no. 7, pp. 1292–1302, 2006.

[9] A. G. Lazaropoulos and P. G. Cottis, "Capacity of overhead medium voltage power line communication channels," *IEEE Transactions on Power Delivery*, vol. 25, no. 2, pp. 723–733, 2010.

[10] A. G. Lazaropoulos and P. G. Cottis, "Broadband transmission via underground medium-voltage power lines—part I: transmission characteristics," *IEEE Transactions on Power Delivery*, vol. 25, no. 4, pp. 2414–2424, 2010.

[11] A. G. Lazaropoulos and P. G. Cottis, "Broadband transmission via underground medium-voltage power lines—part II: capacity," *IEEE Transactions on Power Delivery*, vol. 25, no. 4, pp. 2425–2434, 2010.

[12] P. S. Henry, "Interference characteristics of broadband power line communication systems using aerial medium voltage wires," *IEEE Communications Magazine*, vol. 43, no. 4, pp. 92–98, 2005.

[13] S. Liu and L. J. Greenstein, "Emission characteristics and interference constraint of overhead medium-voltage Broadband Power Line (BPL) systems," in *Proceedings of the IEEE Global Telecommunications Conference (GLOBECOM '08)*, pp. 2921–2925, New Orleans, La, USA, December 2008.

[14] D. Fenton P. Brown, "Modelling cumulative high frequency radiated interference from power line communication systems," in *Proceedings of the IEEE International Conference Power Line Communications and Its Applications*, Athens, Greece, March 2002.

[15] M. Götz, M. Rapp, and K. Dostert, "Power line channel characteristics and their effect on communication system design," *IEEE Communications Magazine*, vol. 42, no. 4, pp. 78–86, 2004.

[16] M. Zimmermann and K. Dostert, "A multipath model for the powerline channel," *IEEE Transactions on Communications*, vol. 50, no. 4, pp. 553–559, 2002.

[17] S. Galli and O. Logvinov, "Recent developments in the standardization of power line communications within the IEEE," *IEEE Communications Magazine*, vol. 46, no. 7, pp. 64–71, 2008.

[18] L. Lampe, R. Schober, and S. Yiu, "Distributed space-time coding for multihop transmission in power line communication networks," *IEEE Journal on Selected Areas in Communications*, vol. 24, no. 7, pp. 1389–1400, 2006.

[19] A. G. Lazaropoulos, "Broadband transmission and statistical performance properties of overhead high-voltage transmission networks," *Journal of Computer Networks and Communications*, vol. 2012, Article ID 875632, 16 pages, 2012.

[20] A. G. Lazaropoulos, "Broadband transmission characteristics of overhead high-voltage power line communication channels," *Progress in Electromagnetics Research B*, vol. 36, pp. 373–398, 2012.

[21] A. G. Lazaropoulos, "Towards broadband over power lines systems integration: transmission characteristics of underground low-voltage distribution power lines," *Progress in Electromagnetics Research B*, vol. 39, pp. 89–114, 2012.

[22] T. Sartenaer, *Multiuser communications over frequency selective wired channels and applications to the powerline access network [Ph.D. dissertation]*, Université Catholique de Louvain, Louvain-la-Neuve, Belgium, 2004.

[23] T. Sartenaer and P. Delogne, "Deterministic modeling of the (shielded) outdoor power line channel based on the Multiconductor Transmission Line equations," *IEEE Journal on Selected Areas in Communications*, vol. 24, no. 7, pp. 1277–1291, 2006.

[24] T. Sartenaer and P. Delogne, "Powerline cables modelling for broadband communications," in *Proceedings of the IEEE International Conference Power Line Communications and Its Applications*, pp. 331–337, Malmö, Sweden, April 2001.

[25] S. Galli, A. Scaglione, and Z. Wang, "For the grid and through the grid: the role of power line communications in the smart grid," *Proceedings of the IEEE*, vol. 99, no. 6, pp. 998–1027, 2011.

[26] T. Calliacoudas and F. Issa, "'Multiconductor transmission lines and cables solver', an efficient simulation tool for plc channel networks development," in *Proceedings of the IEEE International Conference on Power Line Communications and Its Applications*, Athens, Greece, March 2002.

[27] S. Galli and T. C. Banwell, "A deterministic frequency-domain model for the indoor power line transfer function," *IEEE Journal on Selected Areas in Communications*, vol. 24, no. 7, pp. 1304–1315, 2006.

[28] S. Galli and T. Banwell, "A novel approach to the modeling of the indoor power line channel—part II: transfer function and its properties," *IEEE Transactions on Power Delivery*, vol. 20, no. 3, pp. 1869–1878, 2005.

[29] F. Versolatto and A. M. Tonello, "An MTL theory approach for the simulation of MIMO power-line communication channels," *IEEE Transactions on Power Delivery*, vol. 26, no. 3, pp. 1710–1717, 2011.

[30] C. R. Paul, *Analysis of Multiconductor Transmission Lines*, John Wiley & Sons, New York, NY, USA, 1994.

[31] J. A. B. Faria, *Multiconductor Transmission-Line Structures: Modal Analysis Techniques*, John Wiley & Sons, New York, NY, USA, 1994.

[32] H. Meng, S. Chen, Y. L. Guan et al., "Modeling of transfer characteristics for the broadband power line communication channel," *IEEE Transactions on Power Delivery*, vol. 19, no. 3, pp. 1057–1064, 2004.

[33] S. Galli, "A novel approach to the statistical modeling of wireline channels," *IEEE Transactions on Communications*, vol. 59, no. 5, pp. 1332–1345, 2011.

[34] S. Galli, "A simplified model for the indoor power line channel," in *Proceedings of the IEEE International Symposium on Power Line Communications and its Applications (ISPLC'09)*, pp. 13–19, Dresden, Germany, April 2009.

[35] S. Galli, "A simple two-tap statistical model for the power line channel," in *Proceedings of the 14th Annual International Symposium on Power Line Communications and its Applications (IEEE ISPLC '10)*, pp. 242–248, Rio de Janeiro, Brazil, March 2010.

[36] ITU-T SG15/Q4, Powerline channel data, Contribution NIPP-NAI-2007-107R1, 2007.

[37] B. O'Mahony, "Field testing of high-speed power line communications in North American homes," in *Proceedings of the IEEE International Symposium on Power Line Communications and Its Applications (ISPLC '06)*, pp. 155–159, Orlando, Fla, USA, March 2006.

[38] F. Versolatto and A. M. Tonello, "Analysis of the PLC channel statistics using a bottom-up random simulator," in *Proceedings of the 14th Annual International Symposium on Power Line*

*Communications and its Applications (IEEE ISPLC '10)*, pp. 236–241, Rio de Janeiro, Brazil, March 2010.

[39] A. M. Tonello, F. Versolatto, and C. Tornelli, "Analysis of impulsive UWB modulation on a real MV test network," in *Proceedings of the IEEE International Symposium on Power Line Communications and Its Applications (ISPLC '11)*, pp. 18–23, Udine, Italy, April 2011.

[40] M. Antoniali, A. M. Tonello, M. Lenardon, and A. Qualizza, "Measurements and analysis of PLC channels in a cruise ship," in *Proceedings of the IEEE International Symposium on Power Line Communications and Its Applications (ISPLC '11)*, pp. 102–107, Udine, Italy, April 2011.

[41] A. M. Tonello and F. Versolatto, "Bottom-up statistical PLC channel modeling—part II: inferring the statistics," *IEEE Transactions on Power Delivery*, vol. 25, no. 4, pp. 2356–2363, 2010.

[42] P. Amirshahi, *Broadband access and home networking through powerline networks [Ph.D. dissertation]*, Pennsylvania State University, University Park, Pa, USA, 2006.

[43] F. Issa, D. Chaffanjon, E. P. de la Bâthie, and A. Pacaud, "An efficient tool for modal analysis transmission lines for PLC networks development," in *Proceedings of the IEEE International Conference Power Line Communications and Its Applications*, Athens, Greece, March 2002.

[44] J. Anatory and N. Theethayi, "On the efficacy of using ground return in the broadband power-line communications—a transmission-line analysis," *IEEE Transactions on Power Delivery*, vol. 23, no. 1, pp. 132–139, 2008.

[45] N. Theethayi, *Electromagnetic interference in distributed outdoor electrical systems, with an emphasis on lightning interaction with electrified railway network [Ph.D. dissertation]*, Uppsala University, Uppsala, Sweden, 2005.

[46] T. A. Papadopoulos, B. D. Batalas, A. Radis, and G. K. Papagiannis, "Medium voltage network PLC modeling and signal propagation analysis," in *Proceedings of the IEEE International Symposium on Power Line Communications and Its Applications (ISPLC '07)*, pp. 284–289, Pisa, Italy, March 2007.

[47] M. D'Amore and M. S. Sarto, "A new formulation of lossy ground return parameters for transient analysis of multiconductor dissipative lines," *IEEE Transactions on Power Delivery*, vol. 12, no. 1, pp. 303–314, 1997.

[48] P. Amirshahi and M. Kavehrad, "Medium voltage overhead power-line broadband communications; transmission capacity and electromagnetic interference," in *Proceedings of the 9th International Symposium on Power Line Communications and Its Applications (ISPLC '05)*, pp. 2–6, Vancouver, Canada, April 2005.

[49] M. D'Amore and M. S. Sarto, "Simulation models of a dissipative transmission line above a lossy ground for a wide-frequency range—part I: single conductor configuration," *IEEE Transactions on Electromagnetic Compatibility*, vol. 38, no. 2, pp. 127–138, 1996.

[50] M. D'Amore and M. S. Sarto, "Simulation models of a dissipative transmission line above a lossy ground for a wide-frequency range—part II: multiconductor configuration," *IEEE Transactions on Electromagnetic Compatibility*, vol. 38, no. 2, pp. 139–149, 1996.

[51] J. R. Carson, "Wave propagation in overhead wires with ground return," *Bell System Technical Journal*, vol. 5, pp. 539–554, 1926.

[52] H. Kikuchi, "Wave propagation along an infinite wire above ground at high frequencies," *Electrotechnical Journal of Japan*, vol. 2, pp. 73–78, 1956.

[53] H. Kikuchi, "On the transition form a ground return circuit to a surface waveguide," in *Proceedings of the International Congress on Ultrahigh Frequency Circuits Antennas*, pp. 39–45, Paris, France, October 1957.

[54] P. C. J. M. van der Wielen, *On-line detection and location of partial discharges in medium-voltage power cables [Ph.D. dissertation]*, Technische Universiteit Eindhoven, Eindhoven, The Netherlands, 2005.

[55] OPERA1, D5: Pathloss as a function of frequency, distance and network topology for various LV and MV European powerline networks, IST Integrated Project No 507667, 2005, .pdf.

[56] P. C. J. M. Van Der Wielen, E. F. Steennis, and P. A. A. F. Wouters, "Fundamental aspects of excitation and propagation of on-line partial discharge signals in three-phase medium voltage cable systems," *IEEE Transactions on Dielectrics and Electrical Insulation*, vol. 10, no. 4, pp. 678–688, 2003.

[57] J. Veen, *On-Line signal analysis of partial discharges in medium-voltage power cables [Ph.D. dissertation]*, Technische Universiteit Eindhoven, Eindhoven, The Netherlands, 2005.

[58] E. F. Vance, *Coupling to Cable Shields*, John Wiley & Sons, New York, NY, USA, 1978.

[59] R. Aquilué, *Power line communications for the electrical utility: physical layer design and channel modeling [Ph.D. dissertation]*, Universitat Ramon Llull, Enginyeria I Arquitectura La Salle, Barcelona, Spain, 2008.

[60] A. Cataliotti, A. Daidone, and G. Tinè, "Power line communication in medium voltage systems: characterization of MV cables," *IEEE Transactions on Power Delivery*, vol. 23, no. 4, pp. 1896–1902, 2008.

[61] Nexans Deutschland Industries GmbH & Co. KG—catalogue LV underground power cables distribution cables, 2011.

[62] Tele-Fonika Kable GmbH, Cables and wires, 2008, http://www.jauda.com/upload_file/Katalogi/citi/Telefonika/tfb2008.pdf.

[63] G. J. Anders, *Rating of Electric Power Cables*, IEEE Press, New York, NY, USA, 1997.

[64] J. Anatory, N. Theethayi, R. Thottappillil, M. M. Kissaka, and N. H. Mvungi, "The influence of load impedance, line length, and branches on underground cable power-line communications (PLC) systems," *IEEE Transactions on Power Delivery*, vol. 23, no. 1, pp. 180–187, 2008.

[65] D. A. Tsiamitros, G. K. Papagiannis, and P. S. Dokopoulos, "Earth return impedances of conductor arrangements in multilayer soils—part I: theoretical model," *IEEE Transactions on Power Delivery*, vol. 23, no. 4, pp. 2392–2400, 2008.

[66] D. A. Tsiamitros, G. K. Papagiannis, and P. S. Dokopoulos, "Earth return impedances of conductor arrangements in multilayer soils—part II: numerical results," *IEEE Transactions on Power Delivery*, vol. 23, no. 4, pp. 2401–2408, 2008.

[67] F. Rachidi and S. V. Tkachenko, *Electromagnetic Field Interaction with Transmission Lines: From Classical Theory to HF Radiation Effects*, WIT press, Southampton, UK, 2008.

[68] P. A. A. F. Wouters, P. C. J. M. van der Wielen, J. Veen, P. Wagenaars, and E. F. Wagenaars, "Effect of cable load impedance on coupling schemes for MV power line communication," *IEEE Transactions on Power Delivery*, vol. 20, no. 2, pp. 638–645, 2005.

[69] D. Anastasiadou and T. Antonakopoulos, "Multipath characterization of indoor power-line networks," *IEEE Transactions on Power Delivery*, vol. 20, no. 1, pp. 90–99, 2005.

[70] S. Barmada, A. Musolino, and M. Raugi, "Innovative model for time-varying power line communication channel response evaluation," *IEEE Journal on Selected Areas in Communications*, vol. 24, no. 7, pp. 1317–1326, 2006.

[71] J. A. Dobrowolski, *Microwave Network Design Using the Scattering Matrix*, Artech House, Norwood, Mass, USA, 2010.
[72] R. Mavaddat, *Network Scattering Parameters*, Advanced Series in Circuits and Systems, World Scientific Publishing Company, River Edge, NJ, USA, 2nd edition, 1996.
[73] A. Pérez, A. M. Sánchez, J. R. Regué et al., "Circuital and modal characterization of the power-line network in the PLC band," *IEEE Transactions on Power Delivery*, vol. 24, no. 3, pp. 1182–1189, 2009.
[74] E. Liu, Y. Gao, G. Samdani, O. Mukhtar, and T. Korhonen, "Broadband characterization of indoor powerline channel and its capacity consideration," in *Proceedings of the IEEE International Conference on Communications (ICC '05)*, pp. 901–905, Seoul, Korea, May 2005.
[75] M. Kuhn, S. Berger, I. Hammerström, and A. Wittneben, "Power line enhanced cooperative wireless communications," *IEEE Journal on Selected Areas in Communications*, vol. 24, no. 7, pp. 1401–1410, 2006.
[76] M. Crussière, J. Y. Baudais, and J. F. Hélard, "Adaptive spread-spectrum multicarrier multiple-access over wirelines," *IEEE Journal on Selected Areas in Communications*, vol. 24, no. 7, pp. 1377–1388, 2006.
[77] J. Anatory, N. Theethayi, R. Thottappillil, M. Kissaka, and N. Mvungi, "The effects of load impedance, line length, and branches in typical low-voltage channels of the BPLC systems of developing countries: transmission-line analyses," *IEEE Transactions on Power Delivery*, vol. 24, no. 2, pp. 621–629, 2009.
[78] J. Anatory, N. Theethayi, and R. Thottappillil, "Power-line communication channel model for interconnected networks—part II: multiconductor system," *IEEE Transactions on Power Delivery*, vol. 24, no. 1, pp. 124–128, 2009.
[79] H. Philipps, "Modelling of powerline communications channels," in *Proceedings of the IEEE International Symposium on Power Line Communications and Its Applications*, pp. 14–21, Lancaster, UK, March-April 1999.
[80] M. Tlich, A. Zeddam, F. Moulin, and F. Gauthier, "Indoor power-line communications channel characterization up to 100 MHz—part I: one-parameter deterministic model," *IEEE Transactions on Power Delivery*, vol. 23, no. 3, pp. 1392–1401, 2008.
[81] V. Oksman and S. Galli, "G.hn: the new ITU-T home networking standard," *IEEE Communications Magazine*, vol. 47, no. 10, pp. 138–145, 2009.